This article was downloaded by:
On: *14 January 2011*
Access details: *Access Details: Free Access*
Publisher *Taylor & Francis*
Informa Ltd Registered in England and Wales Registered Number: 1072954 Registered office: Mortimer House, 37-41 Mortimer Street, London W1T 3JH, UK

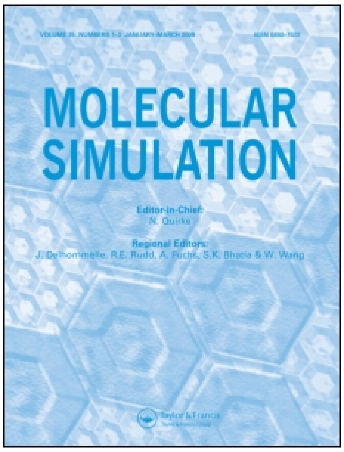

Molecular Simulation

Publication details, including instructions for authors and subscription information:
http://www.informaworld.com/smpp/title~content=t713644482

The Melting Phase Transition in Small Carbon Dioxide Clusters

Jean-Bernard Maillet[a]; Anne Boutin[a]; Alain H. Fuchs[a]

[a] Department of Physical Chemistry, Laboratoire de Chimie-Physique des Matériaux Amorphes, Orsay, France

To cite this Article Maillet, Jean-Bernard , Boutin, Anne and Fuchs, Alain H.(1997) 'The Melting Phase Transition in Small Carbon Dioxide Clusters', Molecular Simulation, 19: 5, 285 — 299

To link to this Article: DOI: 10.1080/08927029708024158

URL: http://dx.doi.org/10.1080/08927029708024158

PLEASE SCROLL DOWN FOR ARTICLE

Full terms and conditions of use: http://www.informaworld.com/terms-and-conditions-of-access.pdf

This article may be used for research, teaching and private study purposes. Any substantial or systematic reproduction, re-distribution, re-selling, loan or sub-licensing, systematic supply or distribution in any form to anyone is expressly forbidden.

The publisher does not give any warranty express or implied or make any representation that the contents will be complete or accurate or up to date. The accuracy of any instructions, formulae and drug doses should be independently verified with primary sources. The publisher shall not be liable for any loss, actions, claims, proceedings, demand or costs or damages whatsoever or howsoever caused arising directly or indirectly in connection with or arising out of the use of this material.

Molecular Simulation, 1997, Vol. 19, pp. 285–299
Reprints available directly from the publisher
Photocopying permitted by license only

THE MELTING PHASE TRANSITION IN SMALL CARBON DIOXIDE CLUSTERS

JEAN-BERNARD MAILLET, ANNE BOUTIN and ALAIN H. FUCHS*

Laboratoire de Chimie-Physique des Matériaux Amorphes, Department of Physical Chemistry, Bâtiment 490, Université Paris-Sud, 91405 Orsay, France

(Received December 1996; Accepted December 1996)

Small isolated carbon dioxide clusters have been studied by canonical and microcanonical Molecular Dynamics simulation. The phenomenon of "dynamical coexistence" between solidlike and liquidlike forms of the $(CO_2)_{13}$ cluster was found, in a finite energy range. An animation of this phenomenon is shown. Coexistence is associated with bimodality in the probability distribution of the short-time averaged internal kinetic energy of the system in the microcanonical ensemble. This phenomenon has also been observed in $(CO_2)_{12,14}$. It is interpreted in terms of the energy distribution of the Potential Energy Surface minima. This statistical mechanics tool enables to understand why dynamical coexistence has also been observed in previous works on $(Ar)_{13}$ and $(N_2)_{13}$ but not in the case of $(Ar)_{8,14}$ and $(SF_6)_{13}$.

Keywords: Small clusters; CO_2; potential energy surface

1. INTRODUCTION

Microscopic van der Waals clusters have received considerable attention in the past two decades [1], as they are believed to provide a mean to understand how the properties of the bulk matter progressively emerge from the atomic behaviour. Small rare gas clusters are known to exhibit non crystalline packing. Farges and coworkers [2] have demonstrated that argon clusters have polyicosahedral then multishell icosahedral form which persist up to a thousand atoms, a size at which it begins to adopt the face-centered cubic (fcc) structure of the bulk material. Comparatively less information is available on the behaviour of polyatomic molecular clusters which are known to exhibit a richer diversity of structures and dynamics than simple

---

*Author to whom correspondence should be addressed.

atomic systems. In previous works on molecular systems, we have shown that the crossover from non crystalline to crystalline bulklike structures occurs in the size range 13 to 19 molecules for sulphur hexafluoride clusters [3, 4], and between 25 and 32 molecules for carbon dioxide clusters [5]. An estimate of the onset of crystalline behaviour for nitrogen is a few hundred molecules [6]. This dramatic difference in behaviour between atomic and polyatomic systems has been attributed to the anisotropy of the repulsive part of the intermolecular potential [3].

Irregular size dependencies were observed by computer simulations in the structural and thermodynamic properties of small Lennard-Jones (LJ) clusters, in the size range of ten to a few hundred atoms [7, 8]. This is clearly related to the fact that certain "magic numbers" of identical atoms may form compact icosahedral structures. In addition $(LJ)_N$ clusters of several sizes ($N = 7, 11, 13, 19, 55,..$) were shown to display a melting phase transition apparently quite unlike the bulk one. Instead of showing two phases coexisting in contact, a "dynamical coexistence" phenomenon was found, in a finite range of energy, between solidlike and liquidlike forms of the clusters [9]. Melting with dynamical coexistence has also been found in polyatomic systems such as $(H_2O)_8$ and $(H_2O)_{20}$ [10] and recently in $(N_2)_{13}$ [11], but not in $(SF_6)_N$ clusters, $N = 7-55$ [2].

Many aspects of the thermodynamics of clusters are still not well understood. For instance, the mechanism of the icosahedral to crystalline transformation, as the number of molecules increases, is unknown [12]. Also some questions regarding the coexistence melting phenomenon remain open, although it has been well characterized in LJ systems [13]. For some times this phenomenon was thought of as "a new kind of phase change" [14]. Later on several theoretical studies have shown that it should rather be understood as the microscopic finite size system analogue of the bulk first-order melting transition [8, 15–18]. Thus the dynamical coexistence must, at some stage, turn into a static coexistence as N increases. Not much is known about the mechanism of this transformation [18]. It is also unclear whether or not the transformations mentioned above (the icosahedral to crystalline and the dynamical to static coexistence melting processes) take place in the same cluster size range (*i.e.* to what extent are these phenomena coupled together?).

We have undertaken an extensive study of carbon dioxide clusters, in which we characterize the dynamics and thermodynamics changes in terms of the underlying Potential Energy Surface (PES) of the system. The size dependency of the PES topography will make it possible to better understand how the bulk phase diagram emerges from the small clusters regime behaviour. In this first paper, we report molecular dynamic simulations of $(CO_2)_{12,13,14}$. We examine the structure and melting processes and relate the observed behaviours to the energy distribution of the minima in the PES. In a forthcoming paper we shall describe the changes in structural, dynamics and thermodynamics of the clusters in the size range ($N = 19-35$) in which the crossover from icosahedral to crystalline behaviour takes place [19].

The complexity of the PES clearly depends on the size of the cluster (the number of structurally distinct minima is thought to grow exponentially with the number of species in the cluster [20, 28]). This is the reason why we have chosen the carbon dioxide molecule for this study. The fact that the crossover point from icosahedral to crystalline behaviour in this system is quite low makes it possible to investigate in details the change in the topography of the cluster's PES by computer simulations.

2. SIMULATION DETAILS

Molecular dynamic simulations were performed using an effective intermolecular potential proposed for bulk CO_2 [21] and used in previous clusters simulations [5, 22]. It consists in an electrostatic interaction term produced by five collinear partial charges located on the symmetry axis of each molecule, plus an atom-atom term of the Lenar-Jones (6–12) form. The ten parameters of the potential function are given in Table I. No boundary conditions were used. Both microcanonical and canonical trajectories were generated, the latter by using Nosé thermostat algorithm

TABLE I Lennard-Jones parameters of the potential function for CO_2 and location of the five partial charges of the molecule [21]. z represents the coordinate along the molecule axis, the origin is the carbon atom. The C—O bond length is 1.16 Å

Lennard-Jones parameters	ε(K)	σ(Å)
C—C	26.3	2.824
O—O	75.2	3.026
partial charges	z(Å)	q(lel)
1	−1.5232	0.1216
2	−1.0663	−0.6418
3	0	−1.0404
4	1.0663	−0.6418
5	1.5232	0.1216

[23] with a coupling Q parameter of 10 kJ$\cdot$mol$^{-1}\cdot$ps. The positions and quaternions coordinates were time stepped using the Beeman algorithm [24]. This time-step algorithm is accurate to the same level of approximation as the more commonly used Verlet algorithm for position, but also for velocity integration step. This is very useful when using a thermostat algorithm in a canonical simulation. A time-step of 5.0 fs was used. At a given temperature, equilibration runs of $\sim$ 200 ps runs were performed, followed by 500 ps to 1 ns production runs performed in both the canonical and microcanonical ensembles. MD runs were performed at different temperature and energy values, from which the stable minima of the Potential Energy Surface (PES) were searched by using the Dynamic Quenching Method (DQM). DQM is similar in nature to the steepest descent method, which was first used in molecular dynamics by Stillinger *et al.* [25, 26]. It consists in applying a frictional damping factor on both force and torque terms in the equations of motion of each molecule [27, 28]. DQM was chosen rather than the more commonly used conjugate gradient technique because we were using a (transputer-based) parallel computer in which dynamics algorithm can be more efficiently implemented. Moreover, the advantage of the DQM over the steepest descent or the conjugate gradient technique, is that the probability of finding a particular minimum depends not only on its width but also on its depth. Thus a narrow and deep well will have a larger appearance frequency using the DQM method.

3. RESULTS

3.1. Structure and Dynamics of $(CO_2)_{13}$ Cluster

Canonical and microcanonical MD runs have been performed on $(CO_2)_{13}$ cluster. A initial configuration was created in a cubic bulklike structure. The fcc structure turned out to be unstable and an instantaneous rearrangement from cubic to icosahedral structure took place in the first ps of the simulation at 5 K. The system was then gradually heated up to 110 K, above its melting point (no evaporation took place during these relatively short runs), and then cooled down, back to the initial temperature using canonical simulations. No hysteresis was found in the caloric curve.

Roughly 1000 quenches have been performed starting from configurations picked up every 5 ps along a trajectory at 100 K in the liquid state. The energy distribution of the PES minima is shown in Figure 1. The global minimum is found at a potential energy of -13.3408 kJ$\cdot$mol^{-1} per molecule.

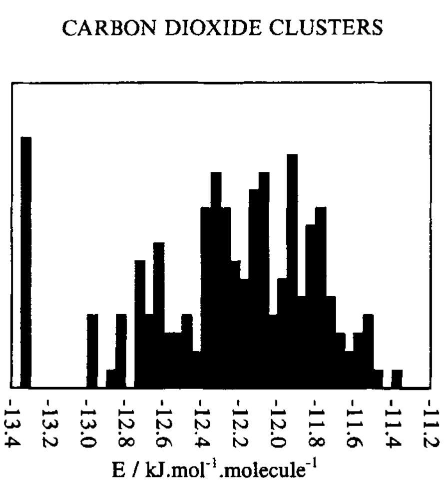

FIGURE 1 Energy distribution of the PES minima of $(CO_2)_{13}$ obtained from ~ 1000 MD quenches. The global minimum is a regular icosahedral structure (point group $\bar{3}$, see text).

The point group is $\bar{3}(i, C_3, C_3^2, S_6, S_6^5)$, and the molecular centres of mass form a regular icosahedron (Fig. 2). An energy gap is observed in the energy distribution of the PES minima. All the other (higher energy) local minima correspond to loosely bound (amorphous) structures. They are associated with the liquid state.

The caloric curve $E(T)$ and the corresponding molar heat capacity, calculated from energy fluctuations in the canonical runs, are shown in Figure 3. Both curves indicate the melting event at $T \approx 90$ K. A bimodal distribution is observed, in a finite range of energy corresponding to melting, in the probability distribution of the short-time averaged internal kinetic energy of the system in the microcanonical ensemble (Fig. 4). The two maxima in this distribution function are plotted in Figure 3a (triangles). Coexistence is observed between the solidlike and liquidlike forms (in much the same way as is LJ_{13} [8]). The coexisting states correspond to liquidlike and solidlike structures respectively. The animation shown below illustrates this phenomenon. Following the Berry and Wales suggestion [8], the dynamical coexistence phenomenon is tentatively associated with the existence of an energy gap between the solid and liquid-like minima in the PES. At low energy the cluster is trapped in the solidlike local minimum. In the intermediate energy range, the system begins to visit the higher energy minima. It jumps back and forth from the global (icosahedral) minimum to the distribution of loosely bound high energy structures which correspond to the liquid state. This process corresponds to the dynamical coexistence phenomenon. At sufficiently higher energy, the system is in the liquidlike state: it mainly explores the distribution of high energy amorphous minima.

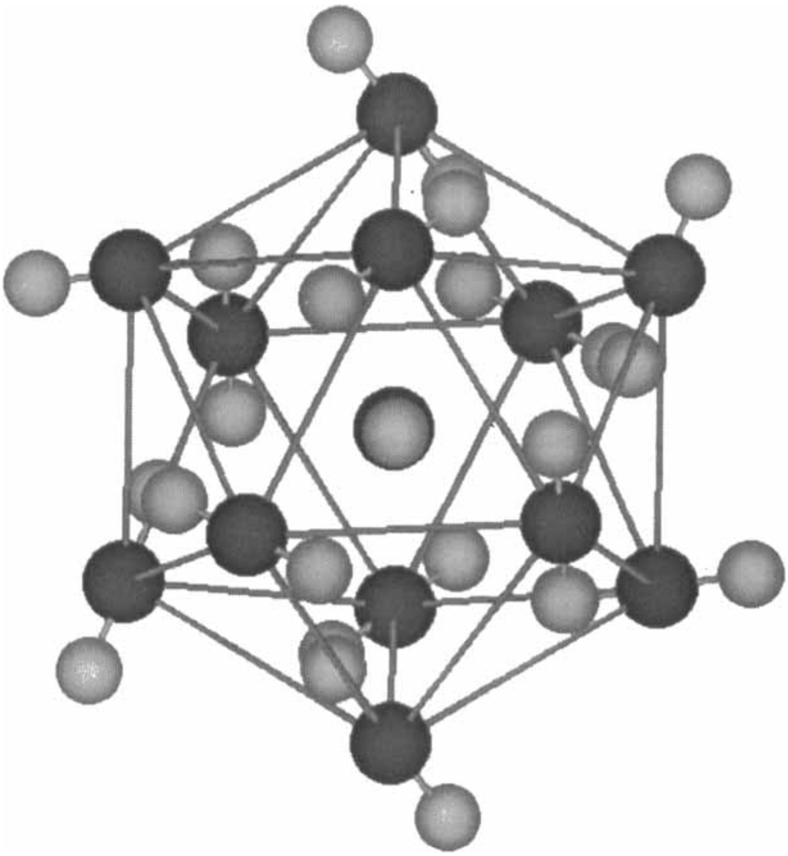

FIGURE 2 The structure of the global minimum in the PES for $(CO_2)_{13}$.

In the microcanonical caloric curve, melting is characterized by a more abrupt change in the slope of $E(T)$, and it takes place in a narrower temperature range, than in the canonical ensemble. Still the microcanonical caloric curve exhibits an inflexion rather than the expected S-bend, for reasons that are presumably similar to the $(LJ)_{13}$ case [8, 9].

Figure 3c displays the computed change in translational (Lindemann's δ) and orientational ($\cos\theta$) order parameters with temperature for $(CO_2)_{13}$. Clearly the translational and orientational degrees of freedom are both released at $T \approx 90$ K, in contrast with $(N_2)_{13}$ in which an orientational transition was observed at low temperature, followed by a translational melting at higher temperature. This has been interpreted in terms of the existence of a finite size analogue of the bulk rigid to plastic phase transition, which is known to occur in solid N_2 but not in CO_2 [11].

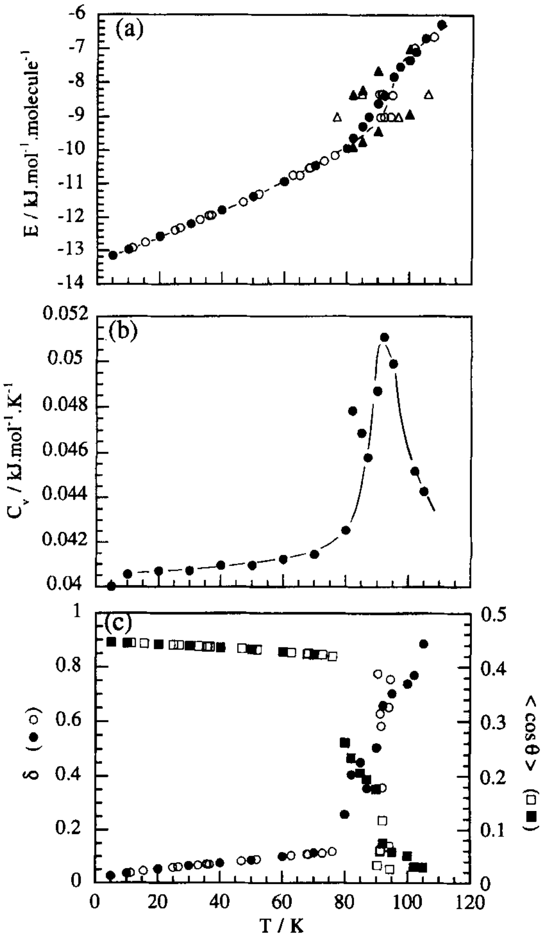

FIGURE 3 Thermodynamics of the $(CO_2)_{13}$ cluster: Open and full symbols correspond to microcanonical and canonical runs, respectively. (a) The caloric curve. Circles correspond to long time averages. Triangles correspond to the stable solidlike and liquidlike forms between which the dynamical coexistence phenomenon is observed. The solid line is a guide to the eye. (b) Molar heat capacity computed from the energy fluctuations in the canonical MD runs. The solid line is a guide to the eye. (c) The orientational (cos θ) and translational (relative root-mean-square intermolecular separation, δ) order parameters as a function of temperature. The definitions of these well known order parameters can be found in [11].

Animation: The Dynamical Coexistence Melting Phenomenon in $(CO_2)_{13}$

The animation displays a series of instantaneous configurations of the $(CO_2)_{13}$ cluster picked up every 0.1 ps during a canonical MD run at $T = 90$ K. During the 45 ps sample shown in the animation the cluster

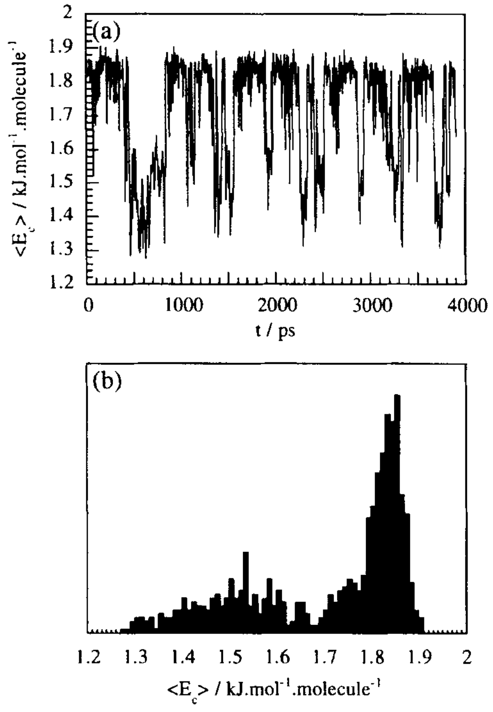

FIGURE 4 (a) Internal kinetic energy as a function of time for $(CO_2)_{13}$ during a microcanonical run of 4 ns at a total energy of 9.02 $kJ \cdot mol^{-1}$. $molecule^{-1}$. The energy is averaged over a period of 1000 steps in order to reduce the vibrational noise. (b) Distribution of short-time-avaraged internal kinetic energy for the same run using a period of 1000 steps.

experiences a solid-liquid transition followed by the reverse freezing of the cluster, thus illustrating the dynamical coexistence phenomenon.

In the beginning of the run, the cluster is icosahedral ($\bar{3}$ structure, on average, see above). To help recognising the icosahedral structure, the central molecule is represented in a different colour and connections are drawn between the first neighbour surface molecular centres of mass. The circle drawn around the cluster represents the sphere in which the solid cluster (averaged over the vibrational-rotational motion fluctuations) is inscribed. In the upper left corner is shown the total cluster energy as a function of time.

In the first 26 ps of the run, the cluster remains in the same, solidlike, structure as evidenced by the total energy fluctuating around a constant value. Despite the considerable rotational-vibrational fluctuations, the icosahedral structure can be identified by the fact that the symmetry axis

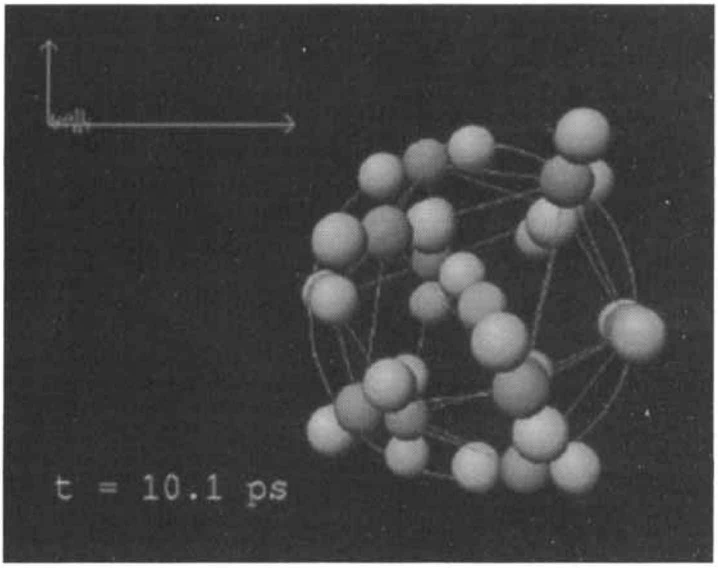

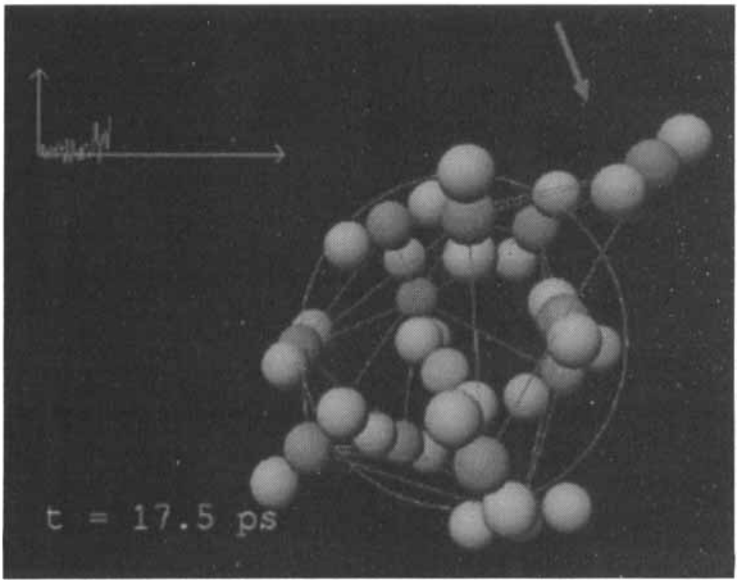

obtained by aligning the central molecule with two surface molecules is five-fold (on average).

After 26.5 ps, one surface molecule indicated by an arrow in the animation (upper right side of the cluster) experiences a significant translational fluctuation and tends to move away from the cluster. This is

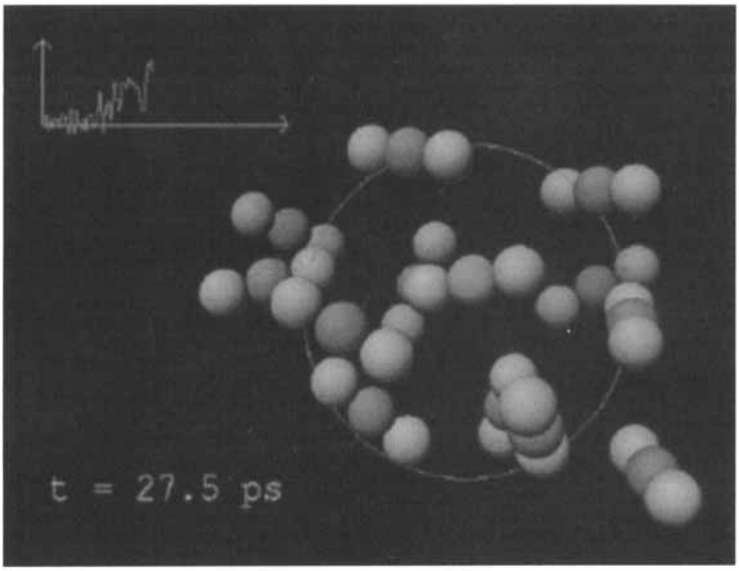

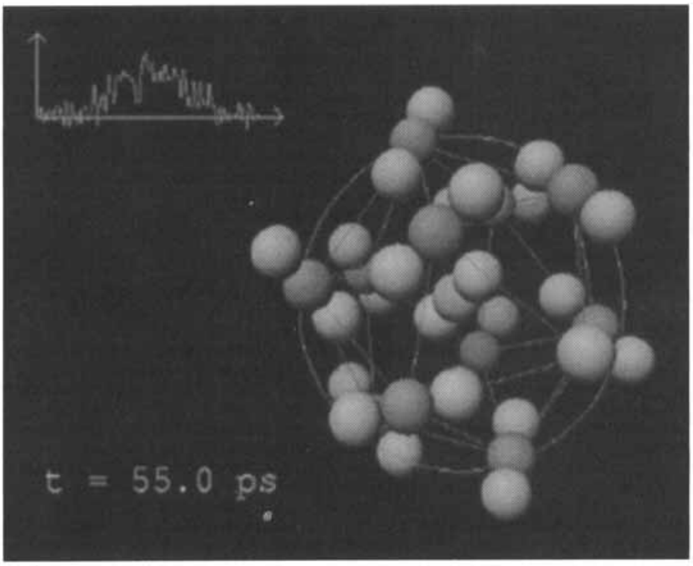

immediately followed by the solid-liquid transition. The liquidlike state of the cluster is characterized by a higher average total energy and by a lower density (as evidenced by the fact that the surface molecules move outside the fixed circle corresponding to the sphere in which the solid cluster was previously inscribed).

The cluster remains in the liquidlike state for ~16 ps. During this time interval, it can be noticed that the former central molecule experiences a brownian translational motion from the centre of the cluster to the surface, and then back to the central position. Because of this diffusional motion, the connections between the surface molecules were not drawn anymore.

Between $t \approx 38$ and 44 ps, the cluster seems to be "searching" a more compact structure. It takes some 6 ps for the cluster to rearrange and find its lower energy state corresponding to the initially solid structure.

3.2. Structure and Dynamics of $(CO_2)_{12,14}$ Clusters

A stated above, coexistence was not always observed in LJ clusters. For instance, $(LJ)_{8,14}$ did not show coexistence while $(LJ)_{7,13}$ did [7, 9, 14]. Here

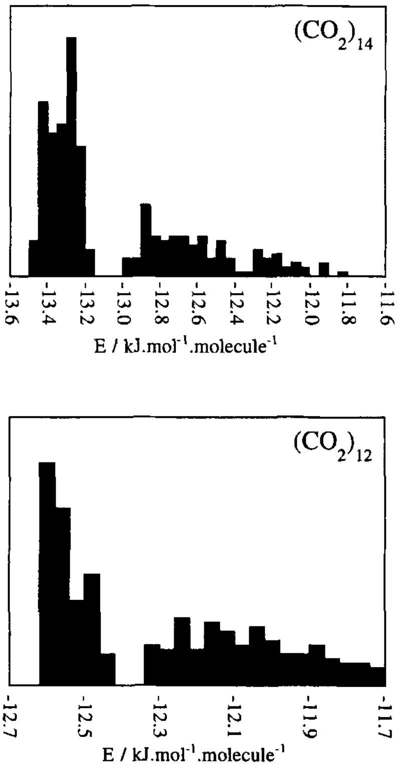

FIGURE 5 Energy distribution of the PES minima of $(CO_2)_{12,14}$ obtained from ~ 1000 MD quenches.

we have studied $(CO_2)_{12,14}$ in order to start investigating the size effect on coexistence in carbon dioxide clusters, and relate the coexistence phenomenon to the properties of the PES.

The energy distribution of the PES minima for these two clusters are shown in Figure 5. Instead of a single global minimum, as in $(CO_2)_{13}$ the PES display a distribution of low energy minima corresponding to defective icosahedral structures. In the case of $(CO_2)_{12}$ the low-lying wells correspond to quasi degenerate rearrangements of icosahedron in which one surface molecule is missing. In the case of $(CO_2)_{14}$ the low-lying minima correspond to rearrangements of capped icosahedron. In both cases we observe a gap in energy between the low energy wells and the distribution of liquidlike high energy minima.

The caloric curves $E(T)$ for $(CO_2)_{12,14}$ are shown in Figure 6. Melting occurs in the range ~70–90 K for $(CO_2)_{12}$, in the range ~85–95 K for $(CO_2)_{14}$. The bimodal behaviour in the probability distribution of the short-time averaged internal kinetic energy in the microcanonical ensemble (or total energy in the canonical ensemble) is also observed in the melting range (Fig. 7). The above mentioned correlation between dynamical coexistence and the existence of an energy gap in the PES seems to be confirmed.

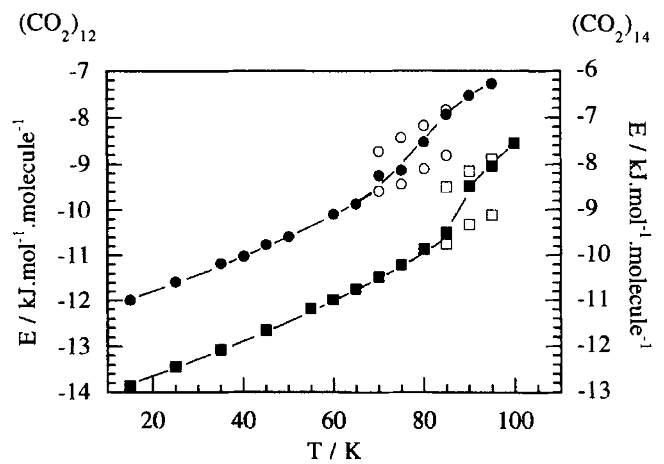

FIGURE 6 Caloric curves of $(CO_2)_{12,14}$ clusters, circles correspond to $N=12$, squares to $N=14$. Full symbols correspond to long time averages. Open symbols correspond to the stable solidlike and liquidlike forms between which coexistence is observed. The solid line is a guide to the eye.

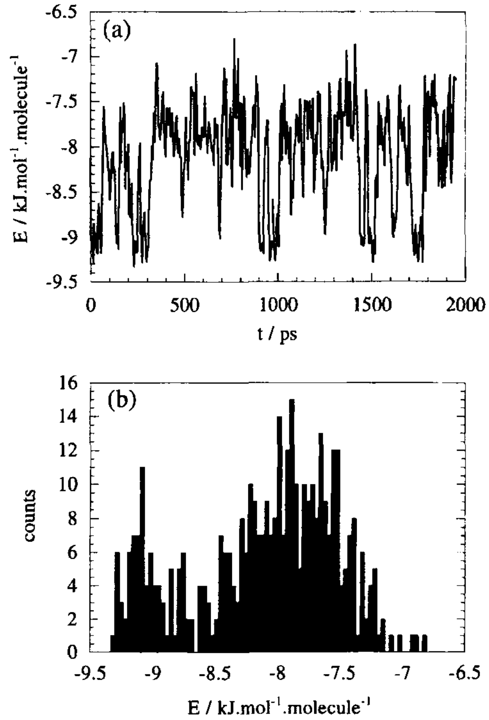

FIGURE 7 (a) Total energy as a function of time for $(CO_2)_{14}$ during a canonical run of 2 ns at $T = 95$ K. The energy is averaged over a period of 1000 steps in order to reduce the vibrational noise. (b) Distribution of short-time-averaged total energy for the same run using a period of 1000 steps.

4. CONCLUSION

Coexistence, characterized by a bimodal distribution in the probability distribution of the short-time averaged internal energy of the system has been observed for $(CO_2)_{12,13,14}$. This is interpreted in terms of the energy distribution of the PES minima.

Clusters for which an energy gap exists between the low energy solidlike minima and the distribution of high energy minima associated with liquidlike state may experience a dynamical coexistence (provided that the energy barrier between the solidlike and liquidlike states is not too high). In the small size regime, the occurrence of dynamical coexistence may clearly depend on the exact number of molecules in the cluster. Clusters which form one (or a few) compact stable solidlike structures at low temperature, are likely to exhibit dynamical coexistence. This will depend on the geometry and force field of the system.

Coexistence has been observed in the cases of $(LJ)_{13}$ and $(CO_2)_{13}$ for which a single global minimum was found (icosahedron I_h in the case of $(LJ)_{13}$ and $\bar{3}$ point group with the molecular centres of mass forming a regular icosahedron in the cases $(CO_2)_{13}$). In addition to the $\bar{3}$ global minimum, $(N_2)_{13}$ displays a set of five low lying local minima. They correspond to icosahedron from the point of view of the centers of mass, but now the molecules exhibit uncorrelated orientations, so that the central molecule is no more a center of symmetry of the cluster. This set of local minima is separated from the liquidlike minima by an energy gap, so that coexistence is also observed in $(N_2)_{13}$.

Non magic number clusters may also exhibit coexistence, provided that the number of low-lying minima is not too high and that they are separated from the liquidlike minima by an energy gap. This was found in $LJ_{11,15}$ and $(CO_2)_{12,14}$. On the other hand $(SF_6)_{13}$, as in the case of $LJ_{8,14}$, displayed a featureless caloric curve and a unimodal short-time averaged kinetic energy distribution for all energies. The global minimum is amorphous and the centres of mass form a highly distorted icosahedron. A broad distribution of low energy minima corresponding to quasidegenerate rearrangements of the distorted icosahedron was found in the PES, and this explains why coexistence has not been observed in this case [3].

In this work we have been able to understand the structural and thermodynamic (melting) behaviours of small carbon dioxide clusters in terms of the energy distribution of the minima in the PES. In a forthcoming paper we shall use this (and other) statistical mechanics tools in order to describe the changes in structural, dynamics and thermodynamics of the clusters in the size range ($N = 19-35$) in which the crossover from icosahedral to crystalline behaviour takes place [19].

Acknowledgement

We thank the Department of Visualization of the "Institut du Développement et des Ressources en Informatique Scientifique" (IDRIS) of CNRS in Orsay for their help in realizing the animation. Sylvie Therond is especially acknowledged for spending so much time on this animation.

References

[1] Berry, R. S. and Cheng, H. P. (1992). "Phase changes for clusters and for bulk matter" in Physics and chemistry of finite systems: from clusters to crystals, Jena, P. *et al.*, eds. *NATO ASI ser. C*, **374**, 277.

[2] Farges, J., de Feraudy, M.-F., Raoult, B. and Torchet, G. (1983). "Noncrystalline structure of argon clusters. I. Polyicosahedral structure of $(Ar)_N$ clusters, $20 < N < 50$" *J. Chem. Phys.*, **78**, 5067; (1986). "Noncrystalline structure of argon clusters. II. Multilayer icosahedral structure of $(Ar)_N$ clusters, $50 < N < 750$" *J. Chem. Phys.*, **84**, 3491.

[3] Boutin, A., Maillet, J.-B. and Fuchs, A. H. (1993). "Structure and dynamics of simulated $(SF_6)_N$ clusters in the size range $N=7-55$" *J. Chem. Phys.*, **99**, 9944.

[4] Boutin, A., Rousseau, B. and Fuchs, A. H. (1994). "The temperature-size phase diagram of large SF_6 clusters by computer simulation" *Chem. Phys. Lett.*, **218**, 122.

[5] Torchet, G., de Feraudy, M.-F., Boutin, A. and Fuchs, A. H. (1996). "Structural transformation in $(CO_2)_N$ clusters, $N < 100$" *J. Chem. Phys.*, **105**, 3671.

[6] Torchet, G. and de Feraudy, M.-F. unpublished results.

[7] Beck, T. L. and Berry, R. S. (1987). "The interplay of structure and dynamics in the metling of small clusters" *J. Chem. Phys.*, **88**, 3910.

[8] Wales, D. J. and Berry, R. S. (1990). "Melting and freezing of small argon clusters" *J. Chem. Phys.*, **92**, 4283.

[9] Wales, D. J. and Berry, R. S. (1994). "Coexistence in finite systems" *Phys. Rev. Lett.*, **73**, 2875; Kunz, R. E. and Berry, R. S. (1994). " Multiple phase coexistence in finite systems" *Phys. Rev, E*, **49**, 1895; Doye, J. P. K. and Wales, D. J. (1995). " An order parameter approach to coexistence in atomic cluster", *J. Chem. Phys.*, **102**, 9673.

[10] Wales, D. J. and Ohmine, I. (1993). "Rearrangements of model $(H_2O)_8$ and $(H_2O)_{20}$ clusters" *J. Chem. Phys.*, **98**, 7245.

[11] Maillet, J.-B., Boutin, A. and Fuchs, A. H. (1996). "Numerical evidence of an embryonic orientational phase transition in small nitrogen clusters" *Phys. Rev. Lett.*, **76**, 4336.

[12] van de Waal, B. W. (1996). "No evidence for size-dependent icosahedral to fcc structural transition in rare gas clusters" *Phys. Rev. Lett.*, **76**, 1083.

[13] Wales, D. J. (1993). "Coexistence in small inert gas clusters" *Molecular Physics*, **78**, 151.

[14] Beck, T. L., Jellineck, J. and Berry, R. S. (1987). "Rare gas clusters: solid, liquids, slush and magic numbers"*J. Chem. Phys.*, **87**, 545.

[15] Labastie, P. and Whetten, R. L. (1990). "Statistical thermodynamics of the cluster solid-liquid transition" *Phys. Rev. Lett.*, **65**, 1567.

[16] Cheng, H. P., Li, X., Whetten, R. L. and Berry, R. S. (1992). "Complete statistical thermodynamics of the cluster solid-liquid transition" *Phys. Rev. A.*, **46**, 791.

[17] Weerasinghe, S. and Amar, F. G. (1993). "Absolute classical densities of states for very anharmonic systems and applications to the evaporation of rare gas clusters" *J. Chem. Phys.*, **98**, 4967.

[18] Quirke, N. (1988). "The microcrystal melting transition", *Molec. Sim.*, **1**, 207.

[19] Maillet, J.-B., Boutin, A., Buttefey, S. and Fuchs, A. H. (in preparation)

[20] Wales, D. J. (1996). "Structure, dynamics and thermodynamics of clusters: Tales from topographic potential surfaces", *Science*, **271**, 92.

[21] Murthy, C. S., O'Shea, S. F. and McDonald, I. R. (1983). "Electrostatic interactions in molecular crystals. Lattice dynamics of solid nitrogen and carbon dioxide" *Mol. Phys.*, **50**, 531.

[22] Cardini, G., Schettino, V. and Klein, M. L. (1989). "Structure and dynamics of carbon dioxide clusters: a molecular dynamics study" *J. Chem. Phys.*, **90**, 4441.

[23] Nosé, S. (1984). "A unified formulation of the constant temperature molecular dynamics methods" *J. Chem. Phys.*, **81**, 511; (1984). "A molecular dynamics method for simulations in the canonical ensemble" *Mol. Phys.*, **52**, 255.

[24] Beeman, D. (1976). "Some multistep methods for use in molecular dynamics calculations" *J. Comput. Phys.*, **20**, 130.

[25] Stillinger, F. H. and Weber, T. A. (1982). "Hidden structure in liquids" *Phys. Rev. A.*, **25**, 978,

[26] Laviolette, R. A. and Stillinger, F. H. (1985)."Multidimensional geometric aspects of the solid-liquid transition in simple substances" *J. Chem. Phys.*, **83**, 4079.

[27] Weerasinghe, S. and Amar, F. (private communication)

[28] Bertolus, M., Brenner, V., Millié, Ph. and Maillet, J.-B. (1997). "Monte-Carlo Growth method: application to molecular clusters" *Z. Phys. D.*, **39**, 239.